

Detection limits of albedo changes induced by climate engineering

Dian J. Seidel^{1*}, Graham Feingold², Andrew R. Jacobson³ and Norman Loeb⁴

A key question surrounding proposals for climate engineering by increasing Earth's reflection of sunlight is the feasibility of detecting engineered albedo increases from short-duration experiments or prolonged implementation of solar-radiation management. We show that satellite observations permit detection of large increases, but interannual variability overwhelms the maximum conceivable albedo increases for some schemes. Detection of an abrupt global average albedo increase <0.002 (comparable to a -0.7 W m^{-2} reduction in radiative forcing) would be unlikely within a year, given a five-year prior record. A three-month experiment in the equatorial zone (5° N – 5° S), a potential target for stratospheric aerosol injection, would need to cause an -0.03 albedo increase, three times larger than that due to the Mount Pinatubo eruption, to be detected. Detection limits for three-month experiments in 1° (latitude and longitude) regions of the subtropical Pacific, possible targets for cloud brightening, are -0.2 , which is larger than might be expected from some model simulations.

Proposals for deliberate modification of the climate system to counteract anthropogenic climate change are gaining momentum^{1–7}. Prominent among the proposed technological fixes (collectively dubbed climate engineering or geoengineering) is an assortment of sunlight-reflection methods (SRM, also called solar-radiation management or short-wave climate engineering) that includes: injecting reflective particles into the stratosphere; brightening marine stratocumulus clouds in the troposphere; and increasing the reflectivity of the Earth's surface, including vegetated areas, oceans and built environments. Their common aim is to modify Earth's energy balance to maintain an average surface temperature within some acceptable range by increasing planetary albedo (reflectivity) to reduce absorption of incoming short-wave radiation. A growing body of literature addresses scientific, technical, environmental, ethical and legal issues^{1–7}. However, it largely ignores the question: could we detect the impacts of either a planned, publicized or independent, undisclosed climate engineering effort?

The answer depends on the availability and adequacy of global observations and on the background variability of the climate system. Although several workshop and committee reports^{1,2,4} mention the general problem of detecting engineered albedo changes (and one⁷ outlines observational requirements for monitoring incoming and reflected solar radiation), no analysis so far has quantitatively estimated detection limits for engineered albedo changes. Studies have considered detection of temperature (and precipitation⁸) changes that might result from SRM activities using either rough estimates⁷ or model simulations⁸ of the background variability. Because changes in these variables have a direct impact on ecosystems and societies, they are of critical interest in SRM discussions. However, temperature and precipitation can change not only in response to changes in climate forcings, but also because of natural climate variability. Thus detection of albedo changes due to SRM is fundamental to determining the effectiveness of SRM in changing Earth's radiative balance and in causing subsequent changes

in surface climate variables. This analysis uses observations of incoming and outgoing short-wave radiation to estimate detection limits for hypothetical SRM-induced albedo increases in an effort to help frame discussions of potential SRM field experiments and implementation.

Challenges of detecting climate engineering

Detection of albedo changes from SRM, like climate change detection in general, is essentially a signal-to-noise problem. The climate system perturbation must exceed both measurement uncertainty and climate variability. Complications arise from the expectation that SRM signals will have spatial and temporal structure. A large regional albedo increase might occur in an area that is not well observed, might be offset by albedo decreases elsewhere or might not appreciably change the global average. A response might not take place immediately, either because of lags in the climate system or because the engineering activity might involve a gradual change. The activity might not cause a sustained effect because the intervention is short term, because climate system processes damp the initial local signal⁹ or because the system tends to rebalance to maintain a stable global or hemispheric value¹⁰. One can foresee such signal-detection complications arising with the leading SRM proposals:

- marine stratocumulus cloud-brightening effects in one region causing opposite albedo effects nearby due to associated changes in atmospheric dynamics⁹
- aerosol injection into the stratosphere causing a gradual increase in albedo as concentrations increase and a gradual decrease as particles leave the atmosphere
- SRM being attempted in a region lacking long-term observations
- governance mechanisms endorsing SRM experiments whose proposed impact is below some regulatory threshold¹¹ or which are anticipated to be measurable locally but not environmentally significant at larger scales¹²

¹National Oceanic and Atmospheric Administration Air Resources Laboratory, R/ARL, NCWCP, Room 4251, 5830 University Research Court, College Park, Maryland 20740, USA, ²National Oceanic and Atmospheric Administration Earth System Research Laboratory, Chemical Sciences Division (R/CSD2), 325 Broadway, Boulder, Colorado 80305, USA, ³National Oceanic and Atmospheric Administration Earth System Research Laboratory and University of Colorado, Global Monitoring Division, 325 Broadway, Boulder, Colorado 80305, USA, ⁴Mail Stop 420, 21 Langley Boulevard, NASA Langley Research Center, Hampton, Virginia 23681-2199, USA. *e-mail: dian.seidel@noaa.gov

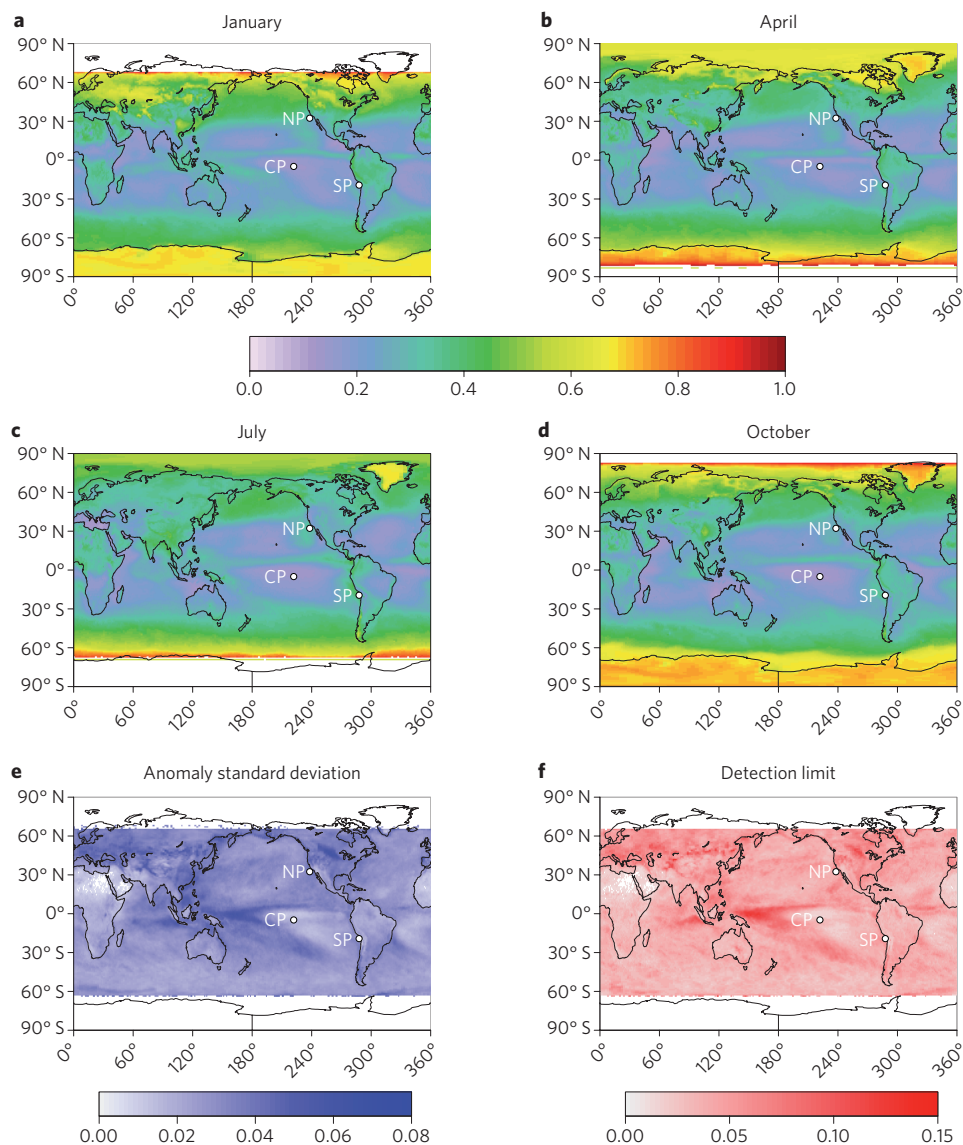


Figure 1 | Albedo climatology and detection limit maps. a–d, Average albedo for the months of January, April, July and October based on 2000–2012 satellite observations of incoming and reflected solar radiation^{14,15}. **e,** Standard deviations of monthly albedo anomalies for the same period. **f,** Detection limit based on a five-year data record before an abrupt, sustained increase in albedo, and a one-year period after. All albedo values are dimensionless ratios (that is, they are not expressed as percentages). CP is the equatorial location, and NP and SP are the northern and southern subtropical locations, respectively.

An approach to SRM detection

This analysis used standard statistical tests and existing observations^{13–15} to estimate detection limits for idealized albedo interventions. We considered detection at both the global and regional scales, distinguished between abrupt, sustained interventions and gradual ramp-up schemes, and assessed how the duration of an experiment influences its detection. Because we used existing data, the analysis could not investigate the effects of potential feedbacks induced by the perturbation. Details regarding data and test procedures are in the Methods section.

Uninterrupted, near-global, high-precision records of incoming and reflected solar radiation measured by satellite-borne instruments are required for detecting SRM activities. Whether the intended albedo increase is at the surface (for example, light versus dark coloured roofs), in the troposphere (cloud brightening) or in the stratosphere (aerosol injection), the goal is to increase reflection from the planet, so space-based measurements are well-suited to the detection problem. We employed albedo computed from the 2000–2012 CERES EBAF Ed2.6r^{13–15} observations to simulate SRM

interventions and to determine how large an intervention must be for it to be detected above the variability of the climate system. The monthly 1° latitude \times 1° longitude ($\sim 10^{10}$ m²) resolution of the data frames the space and time resolution of both this analysis and potential future SRM detection based on these observations.

Patterns of albedo variability

The annual cycle causes the most salient variations in albedo¹⁶ (Fig. 1a–d). At high latitudes, snow and ice accumulation in winter produce the largest seasonal changes (~ 0.4 non-dimensional albedo units), but at lower latitudes, changes in vegetation and cloudiness also cause significant albedo changes (~ 0.2). The amplitude of the annual cycle in global average albedo is 0.03, $\sim 10\%$ of the annual mean value (0.29); see Methods and Fig. 2. We examined two areas of the eastern subtropical Pacific Ocean, each at both $1^\circ \times 1^\circ$ and $5^\circ \times 5^\circ$ resolution, where the annual cycle is a much larger percentage of the annual mean, and a $1^\circ \times 1^\circ$ area of the central equatorial Pacific, where both mean albedo and albedo variability are very low (Fig. 1 and Methods). The amplitude of the annual cycle is ~ 0.10 and 0.25, in the northern

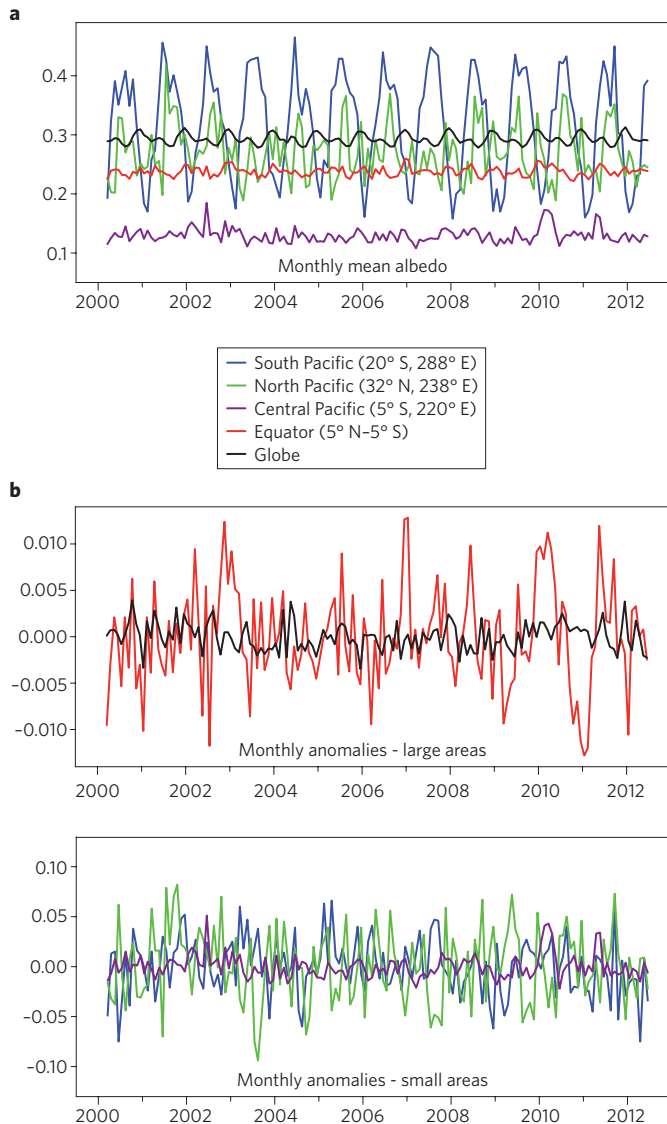


Figure 2 | Global and regional albedo time series. **a, b**, Monthly mean (**a**) and de-seasonalized monthly anomaly (**b**) albedo for 2000–2012, based on satellite observations^{14,15} for the global average, the equatorial belt and regions of the central equatorial Pacific, subtropical South Pacific and North Pacific, all 1° × 1° boxes identified in Fig. 1. Climatological mean values and standard deviations of anomalies for these regions are given in Table 1.

and southern subtropical locations (NP and SP in Fig. 1), respectively, or ~37% and 78% of the annual mean values of 0.27 and 0.32. In the equatorial location (CP in Fig. 1), the annual mean albedo is 0.13, and the amplitude of the annual cycle is ~6% of the mean.

For the purposes of detecting SRM-induced albedo perturbations, these expected seasonal variations can be computed from prior multi-year observations and readily removed. Interannual albedo variations, on the other hand, are generally non-periodic and so constitute noise that must be exceeded for confident detection. The magnitude of interannual variations (as measured by their standard deviation, Fig. 1e) is larger for ocean than for land areas and is greatest where snow and ice vary most (the edges of the polar zones) and where cloud cover varies most (the tropical Pacific and Indian oceans). Among land areas, Africa, the Middle East, the northern part of South America, parts of Southeast Asia and Australia, and some islands in the equatorial western Pacific exhibit relatively low interannual albedo variability (Fig. 1e), and

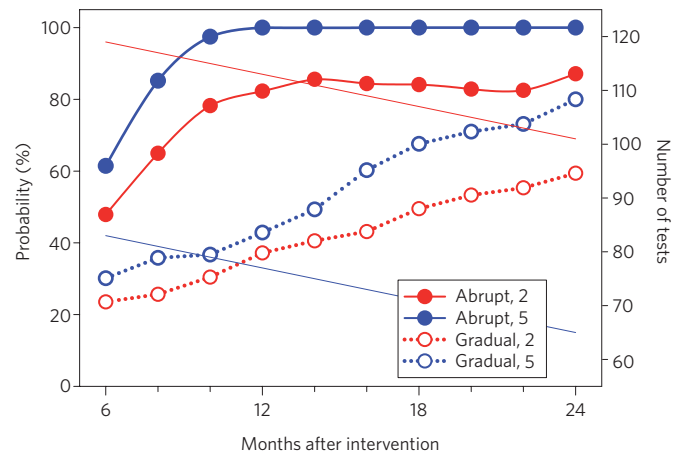


Figure 3 | Global albedo detection probabilities. The probability of detecting a 0.002 increase in global average planetary albedo as a function of the waiting period after intervention, based on monthly albedo anomaly data for 2000–2012 (shown in Fig. 2b). Probabilities are percentages of tests using all possible pairs of consecutive periods of observation. Periods before intervention were either 2 (red) or 5 (blue) years, and periods after intervention ranged from 6 to 24 months. The total number of tests for each pair of periods is shown by the thin lines (right y axis). Imposed albedo changes were either abrupt and sustained (stepwise increase of 0.002 from one month to the next, Type 1 in Methods, filled circles) or gradual (linear increase from 0 to 0.002 over the period after intervention, Type 3 in Methods, open circles). Probability of detection is the percentage of Student’s *t*-tests showing a statistically significant (95% confidence level) increase in mean albedo.

relatively low average albedos (Fig. 1a–d), a combination that might make those regions seem to be good candidates for SRM, for example, by increasing the reflectivity of grasslands^{17,18}.

Monthly albedo anomaly time series (Fig. 2) suggest, and calculations confirm, that there is no significant trend and little shorter-term persistence (autocorrelation) in the 12-year record (see Methods) that would confound detection by either masking or enhancing an engineered effect. These climate-related variations far exceed measurement uncertainty, which we neglect as a source of noise: the standard deviation of global monthly anomalies is 0.0015 (Methods), which is ~2.5 times larger than the 0.0006 one-sigma global uncertainty in monthly mean albedo¹⁵.

Defining global detection probabilities

Although SRM proposals target specific regions, their main aim is to increase global average albedo. Therefore, we first examined detection limits at the global scale. Figure 3 illustrates some general principles and detection probabilities for an engineered 0.002 albedo increase (for example, from 0.293 to 0.295). Such a global change in albedo is comparable to an ~0.7 W m⁻² reduction in radiative forcing. It exceeds the estimated upper limit of albedo changes for SRM proposals involving land surface changes and biological enhancement of marine clouds¹⁷, but is less than the estimated upper limit associated with mechanical enhancement of marine cloud albedo¹⁷ and stratospheric aerosol injection⁴.

We imposed both abrupt and gradual 0.002 perturbations to the 2000–2012 global anomaly time series (Fig. 2), then tested all possible adjacent time intervals, of varying lengths, to estimate the probability of such a change causing a statistically significant increase (see Methods). Abrupt changes (Type 1, described in Methods) could be caused by SRM field experiments of limited duration or by SRM deployment that achieves an immediate albedo change and maintains it for a fixed period or indefinitely.

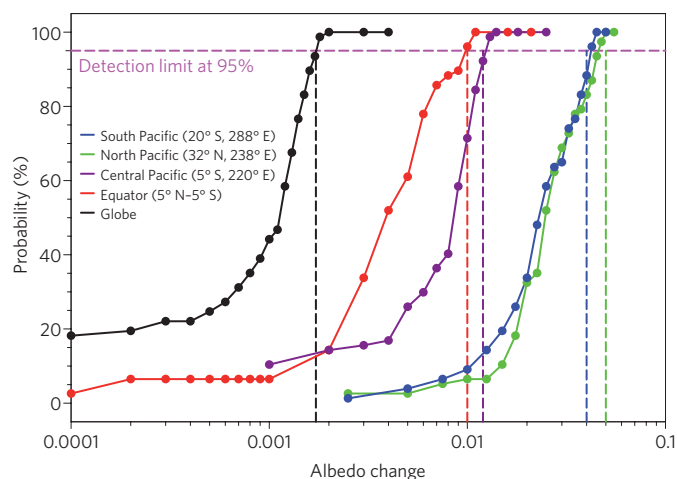


Figure 4 | Regional albedo detection limits. Probabilities of detecting abrupt, sustained albedo increases of varying magnitude within one year, given a five-year prior data record, for the same five regions as in Fig. 2. This study defines detection limits as albedo changes having a 95% probability of detection (dashed lines).

Gradual changes (Type 3 in Methods) could be caused by monitored deployment ramping up to a steady-state intervention⁷.

As seen in Fig. 3, with a five-year observational record before an intervention, a 0.002 increase has a probability of detection P of 60–100% if the intervention is abrupt and sustained (Type 1), and P increases with increasing time (from 6 to 24 months) after initiation of SRM. If the intervention is gradual (Type 3), P ranges between 30% and 80%. In general, P is higher for abrupt changes than gradual ones, at least in part because the time-integrated albedo change is larger in the abrupt case, and for longer waiting periods after intervention. Detection probabilities for a two-year prior record are ~5–20% lower than for five-year records. These results underscore the value of an extant, continuous data record before SRM to characterize pre-intervention average albedo and its variability.

Global and regional detection limits

Using five-year prior records and one-year waiting periods, Fig. 4 shows global and regional detection probabilities for ranges of abrupt, sustained (Type 1) albedo increases. Globally, a 0.0001 change, the estimated¹⁷ effect of changing land surface albedo in urban areas totalling $\sim 10^{12}$ m², has $P < 20\%$. The probability rises to 95% for a perturbation of 0.002, and we define the threshold perturbation at

which $P = 95\%$ as the detection limit. Based on Fig. 4, a 0.006 change in the global average albedo, the estimated¹⁷ effect of increasing land surface albedo in desert areas totalling $\sim 10^{13}$ m² ($\sim 2\%$ of Earth's surface), would be detectable, as would an increase of 0.01, which is large enough to counteract the radiative forcing associated¹⁷ with a doubling of atmospheric carbon dioxide relative to pre-industrial levels.

For albedo change averaged over smaller regions, similarly defined detection limits are much larger (Fig. 4 and Methods). In the 10° latitude equatorial band, it is 0.01, about the magnitude of increase observed in that region in August after the June 1991 eruptions of Mount Pinatubo¹⁹, an oft-cited natural analogue for SRM proposals involving stratospheric aerosols. Assuming no compensating albedo changes outside this region, a 0.01 equatorial albedo increase is equivalent to a ~ 0.002 global increase — the estimated global detection limit.

The two $1^\circ \times 1^\circ$ subtropical marine regions examined have detection limits of 0.04 and 0.05, with a larger limit in the northern subtropical Pacific, due to the higher interannual variability there. A model-estimated 0.4 maximum albedo increase resulting from marine cloud brightening in a clean air mass region²⁰ would be easily detected. However, simulated estimates of the effects of ship tracks on albedo indicate much smaller increases (~ 0.08 , or ~ 0.02 in polluted areas), and only within ~ 200 km of the source of cloud condensation nuclei²¹. If marine cloud brightening were to cause comparable albedo increases, they might not be detectable. Although an ~ 0.04 albedo increase could be detected in a $1^\circ \times 1^\circ$ region, it would change global average albedo by only 0.000001 — three orders of magnitude less than the global detection limit. When these two domains were expanded to $5^\circ \times 5^\circ$ (an area 25 times larger), we obtained very similar measures of variability and the same detection limits (to one significant figure) as for the smaller regions, because the monthly anomaly time series for the larger region closely resembles that of the smaller one.

The spatial pattern of detection limit largely mirrors that of anomaly standard deviation (Fig. 1e,f) and indicates regions where SRM is most and least likely to be detected. At this $1^\circ \times 1^\circ$ resolution, detection limits range over an order of magnitude, from 0.01 (for example, northern Africa and the central equatorial Pacific) to 0.10 (for example, the western equatorial Pacific), highlighting the sensitivity of detection to the choice of test location.

Detectability of field experiments

The possibility of planned, internationally accepted outdoor SRM experiments depends on many factors, most beyond the scope of this discussion. One critical question is: how large an albedo change must be attempted, and for how long, to ensure it will be detectable? Experimenters would probably also want to detect changes in

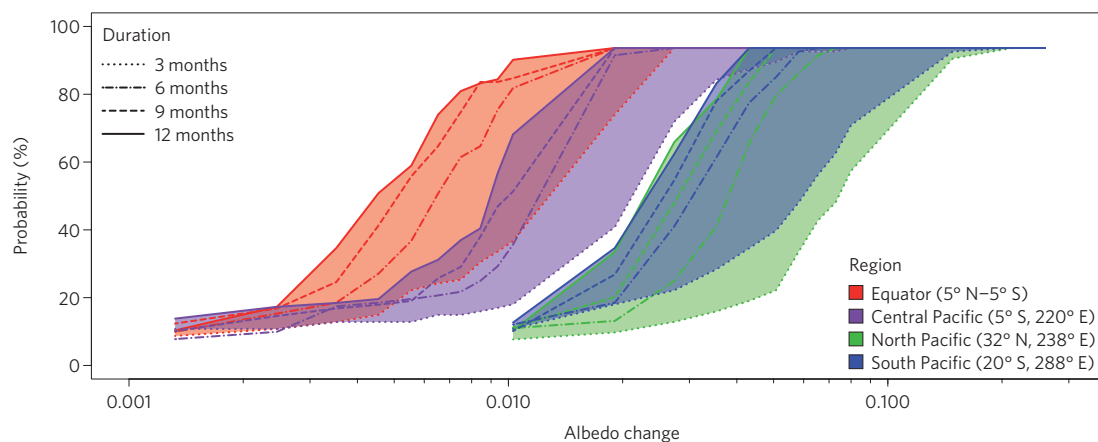


Figure 5 | Detectability of field experiments. Probability of detecting short-term (3–12 month) abrupt, sustained albedo changes of varying magnitudes in four potential test regions: the equatorial belt (5° N– 5° S) and three $1^\circ \times 1^\circ$ Pacific Ocean regions.

Table 1 | Albedo average values, standard deviations of anomalies and detection limits for seven regions. All values are given in non-dimensional albedo units (not as percentages).

	Globe	Equator	Central Pacific (1° × 1°)	North Pacific (1° × 1°)	North Pacific (5° × 5°)	South Pacific (1° × 1°)	South Pacific (5° × 5°)
Annual mean	0.293	0.238	0.130	0.271	0.271	0.318	0.319
January mean	0.303	0.245	0.131	0.264	0.267	0.185	0.216
April mean	0.298	0.243	0.133	0.238	0.239	0.308	0.320
July mean	0.286	0.238	0.129	0.339	0.331	0.413	0.381
October mean	0.293	0.231	0.125	0.263	0.261	0.352	0.345
Annual standard deviation	0.0006	0.0020	0.005	0.010	0.010	0.011	0.008
Monthly standard deviation	0.0015	0.0054	0.012	0.036	0.032	0.028	0.024
Detection limit	0.002	0.01	0.01	0.05	0.05	0.04	0.04
Equivalent global increase	0.002	0.002	0.000003	0.000001	0.00003	0.000001	0.00002

the parameters directly targeted by their experiments (for example, aerosol size and optical properties; cloud fraction and microphysical properties). However, to evaluate the efficacy of an experiment designed to increase reflection of sunlight fundamentally requires detection of a change in albedo. Alternatively, an SRM experiment undertaken without oversight from an agreed-upon governance structure, and possibly without public announcement, could potentially be 'detected' through sightings of people and equipment in action. But that evidence would reveal nothing regarding the potential impact on the energy balance of the climate system, for which the operative question is: would the climate monitoring community, with its current observational capabilities, detect the albedo change?

Figure 5 shows the probability of detecting changes ranging over two orders of magnitude, and sustained for periods of 3, 6, 9 and 12 months, in the equatorial belt (5° N–5° S) and in the same Pacific Ocean regions examined above. As expected, longer experiments, and larger albedo changes, have a greater chance of being detected. Interventions that are highly likely ($P = 95\%$) to be detected in a 12-month experiment, have little chance ($P < 30\%$) in three-month experiments. The detection limit for a three-month Type 1 experiment in the equatorial band is ~ 0.03 . If a small-scale three-month experiment were attempted in the carefully selected 1° × 1° region within this band with low albedo and low variability, the detection limit would be ~ 0.05 . In the 1° × 1° subtropical Pacific Ocean regions, detection limits are ~ 0.2 , about four times larger than in the equatorial region. If such large albedo changes could not be achieved and sustained over a three-month period, it is not likely that SRM experiments could be unambiguously detected in these regions.

The nature of the field experiment influences its likelihood of detection. An intervention that is immediate and sustained over the experimental period (Type 1 intervention) is more likely to be detected than one involving an initial pulse that decays exponentially (Type 2), such as might be expected for stratospheric aerosol injection. Gradually ramping up an albedo increase (Type 3) is even less likely to be detected (Supplementary Fig. S1).

Some caveats and practical implications

These notional SRM detection limits are sensitive to methodological choices. We offer them as initial, practical estimates of the magnitude of albedo effects whose detection is within the realm of possibility. Probability of detection would be smaller if the data windows before or after intervention were shorter or if the required P were higher. Furthermore, because albedo is ill-defined in polar night conditions, we were not able to perform these statistical tests for high latitudes.

More sophisticated approaches to detecting SRM effects on albedo are conceivable and could involve ancillary observations in targeted geographical areas to isolate possible engineered changes. For example, albedo changes over ocean regions from stratospheric aerosol injection might be detected at lower thresholds by employing cloud, tropospheric aerosol, sea ice, surface wind and ocean colour observations to distinguish stratospheric from surface and/or tropospheric changes.

These findings have implications for observing system requirements for future detection of climate engineering, as well as for the broader climate-engineering debate. Continuation of short-wave radiation observations by satellites, at the same level of precision as is now available or better, would probably allow detection of SRM activities exceeding the limits estimated here, if they were of large enough spatial scale. A gap in the data record would confound detection, even if the gap occurred before any intervention. This continuity requirement applies to climate change detection generally²² and is not unique to the problem of detecting climate engineering activities.

With current observations, we would be unlikely to detect any but the most ambitious and effective SRM field experiment or implementation effort, because small effects would be masked by background albedo variability. If we can not unambiguously detect the effects of climate engineering on albedo, we can not ascertain the efficacy of authorized activities, detect surreptitious operations, understand and distinguish among the multiple causes of continuing and projected climate change, predict their effects on key climate variables such as temperature and precipitation, or effectively administer agreements to govern SRM activities. In short, if we can not measure the effects of climate engineering, we can not manage them.

Methods

Albedo data used in this analysis are derived from incoming solar and reflected short-wave fluxes from the Clouds and Earth's Radiant Energy System (CERES) Energy Balanced and Filled (EBAF) Top of the Atmosphere (TOA, Ed2.6r) datasets^{13–15}, obtained from the NASA Langley Research Center CERES ordering tool at <http://ceres.larc.nasa.gov>. Observations are at monthly 1° latitude × 1° longitude resolution from March 2000 to June 2012. These data have been carefully quality controlled and are considered free of time-varying biases that could undermine this analysis¹⁵.

We computed monthly mean albedo for each grid point and month as the ratio of reflected to incoming flux. Anomalies were computed by removing the long-term monthly average from each monthly value. All albedo values (means and anomalies) are dimensionless numbers and are expressed as ratios, not as percentages (as is sometimes done).

Table 1 gives climatological mean albedo (averaged over the 12 years of observation) and standard deviations of the 12 annual values and of monthly anomalies, for five regions used in the analysis: globe, equatorial belt (5° N–5° S), a central

equatorial Pacific Ocean region (5° S, 220° E), a north subtropical Pacific Ocean region (32° N, 238° E) and a south subtropical Pacific Ocean region (20° S, 288° E). Results for the two subtropical Pacific regions are given for 1° × 1° and 5° × 5° domains.

Table 1 also shows estimated one-year detection limits, for an abrupt and sustained increase in albedo, given a five-year prior observational record. Detection limits are reported to one significant figure, in consideration of the assumptions and idealizations made in their estimation. Equivalent global albedo increases are estimated using area-weighted averaging, and by assuming regional albedo increases the same size as the estimated regional detection limit, and zero albedo change elsewhere.

The two regions of the eastern subtropical Pacific Ocean were selected because of recent field experiments^{23,24} that measured marine stratocumulus cloud properties, including albedo, and because these marine stratocumulus clouds have been mentioned as possible targets of brightening efforts²⁰. Similarly, the equatorial zone has been mentioned in the context of stratospheric aerosol injection, another proposed sunlight reflection method, and the 1° × 1° region of the central Pacific was selected because of its low albedo and albedo variability.

Detection limits are based on the results of suites of Student's *t*-tests of means before and after hypothetical climate engineering activities. Non-parametric rank-order tests of medians were also conducted, and they gave identical results in >90% of cases. We employed the *t*-test because the effects of autocorrelation in time series on the number of degrees of freedom can be readily taken into account. Lag-one autocorrelations of monthly albedo anomaly time series are 0.12 and 0.28 for the globe and equatorial belt, respectively, and 0.12, and 0.08 for the 1° × 1° areas of the North Pacific and South Pacific, respectively.

Detection limits are estimated using sets of (at least ten) tests performed for specified observational window lengths before and after an intervention, and for a specified magnitude of intervention. By advancing through a time series of monthly albedo anomalies, all possible pairs of adjacent windows are tested by imposing an intervention (an increase in albedo) on the data in the second window.

If the mean anomaly in the second window is found to be statistically significantly greater (using a one-sided *t*-test, and at the 95% confidence level) from that of the first, we considered this a 'detected' change. Otherwise, the change is too small to be detected above the noise in the time series. If 95% or more of the tests for a given window length pair and intervention resulted in detection, we considered that intervention to be a detectable change. Detection limits were determined by gradually increasing the magnitude of the intervention until a detectable change was found. For context, we compared the estimated detection limits with albedo changes for different proposed climate engineering schemes, estimated by ref. 17.

Three types of intervention were analysed. A Type 1 intervention is an instantaneous albedo increase held constant over the window. A Type 2 intervention is an instantaneous increase followed by an exponential decrease with *e*-folding time equal to the window length. A Type 3 intervention is a gradual linear increase over the window period. The time-integrated albedo change is largest for Type 1 and smallest for Type 3 interventions. Supplementary Fig. S1 shows that Type 1 interventions have a greater probability of detection than Type 2 interventions, which in turn have a greater probability than Type 3.

Received 17 June 2013; accepted 8 November 2013;
published online 29 January 2014; corrected after print
29 January 2014

References

1. Shepherd, J. *Geoengineering the Climate: Science, Governance and Uncertainty* (The Royal Society, 2009).
2. Bipartisan Policy Center's Task Force on Climate Remediation Research *Geoengineering: A National Strategic Plan for Research on the Potential Effectiveness, Feasibility, and Consequences of Climate Remediation Technologies* (Bipartisan Policy Center, 2011); <http://bipartisanpolicy.org/library/report/task-force-climate-remediation-research>

3. *Climate Engineering: Technical Status, Future Directions, and Potential Responses* GAO-11-71 (US Government Accountability Office, 2011); <http://www.gao.gov/assets/330/322208.pdf>
4. Vaughan, N. E. & Lenton, T. M. A review of climate geoengineering proposals. *Climatic Change* **109**, 745–790 (2011).
5. Convention on Biological Diversity *Additional Information on Options for Definitions of Climate-Related Geoengineering* UNEP/CBD/COP/11/INF/2 (UNEP, 2012); <http://www.cbd.int/doc/meetings/cop/cop-11/information/cop-11-inf-26-en.pdf>
6. Belter, C. W. & Seidel, D. J. A bibliometric analysis of climate engineering research. *WIREs Clim. Change* **4**, 417–427 (2013).
7. Blackstock, J. J. *et al.* *Climate Engineering Responses to Climate Emergencies* Preprint at <http://arxiv.org/pdf/0907.5140> (Novim, 2009).
8. MacMynowski, D. G., Keith, D., Caldeira, K. & Shin, H.-J. Can we test geoengineering? *Energ. Environ. Sci.* **4**, 5044–5052 (2011).
9. Stevens, B. & Feingold, G. Untangling aerosol effects on clouds and precipitation in a buffered system. *Nature* **461**, 607–613 (2009).
10. Voigt, A., Stevens, B., Bader, J. & Mauritsen, T. The observed hemispheric symmetry in reflected shortwave irradiance. *J. Clim.* **26**, 468–477 (2013).
11. Parson, E. A. & Keith, D. W. End the deadlock on governance of geoengineering research. *Science* **339**, 1278–1279 (2013).
12. Solar Radiation Management Governance Initiative *Solar Radiation Management: The Governance of Research* (SRMGI, 2011); <http://www.srmgi.org/report>
13. Loeb, N. G. *et al.* Multi-instrument comparison of top-of-atmosphere reflected solar radiation. *J. Clim.* **20**, 575–591 (2007).
14. Loeb, N. G. *et al.* Toward optimal closure of the Earth's top-of-atmosphere radiation budget. *J. Clim.* **22**, 748–766 (2009).
15. Loeb, N. G. *et al.* Advances in understanding top-of-atmosphere radiation variability from satellite observations. *Surv. Geophys.* **33**, 359–385 (2012).
16. Hatzianastassiou, N. *et al.* Long-term global distribution of Earth's shortwave radiation budget at the top of atmosphere. *Atmos. Chem. Phys.* **4**, 1217–1235 (2004).
17. Lenton, T. M. & Vaughan, N. E. The radiative forcing potential of different climate geoengineering options. *Atmos. Chem. Phys.* **9**, 5539–5561 (2009).
18. Hamwey, R. M. Active amplification of the terrestrial albedo to mitigate climate change: an exploratory study. *Mitig. Adapt. Strat. Glob. Change* **12**, 419–439 (2007).
19. Minnis, P. *et al.* Radiative climate forcing by the Mount Pinatubo eruption. *Science* **259**, 1411–1415 (1993).
20. Latham, J. *et al.* Marine cloud brightening. *Phil. Trans. R. Soc. A* **370**, 4217–4262 (2012).
21. Wang, H. & Feingold, G. Modeling mesoscale cellular structure and drizzle in marine stratocumulus. Part II: The microphysics and dynamics of the boundary region between open and closed cells. *J. Atmos. Sci.* **66**, 3257–3275 (2009).
22. Global Climate Observing System *Implementation Plan for the Global Observing System for Climate in Support of the UNFCCC, Executive Summary* GCOS-92 (ES) (WMO/TD No. 1244, World Meteorological Organization, 2004); http://www.wmo.int/pages/prog/gcos/Publications/gcos-92_GIP_ES.pdf
23. Stevens, B. *et al.* Dynamics and chemistry of marine stratocumulus — DYCOMS-II. *Bull. Am. Meteorol. Soc.* **84**, 579–593 (2003).
24. Wood, R. *et al.* The VAMOS ocean-cloud-atmosphere-land study regional experiment (VOCALS-REx): goals, platforms, and field operations. *Atmos. Chem. Phys.* **11**, 627–654 (2011).

Additional information

Supplementary information is available in the [online version of the paper](#). Reprints and permissions information is available at www.nature.com/reprints. Correspondence and requests for materials should be addressed to D.S.

Competing financial interests

The authors declare no competing financial interests.

Detection limits of albedo changes induced by climate engineering

Dian J. Seidel, Graham Feingold, Andrew R. Jacobson and Norman Loeb

Nature Climate Change **4**, 93–98 (2014); published online 29 January 2014; corrected after print 29 January 2014

In the version of this Perspective originally published, the final phrase of the abstract should have read ‘are ~ 0.2 , which is larger than might be expected from some model simulations.’ Additionally, the affiliation number for Norman Loeb was missing in the address list. These errors have been corrected in the online versions of the Perspective.